

## SENSITIVITY ANALYSIS OF MECHANICAL COUPLINGS MODEL APPLYING FREQUENCY RESPONSE FUNCTIONS

**Abdon Tapia Tadeo.**

UNICAMP - Universidade Estadual de Campinas, Departamento de Projeto Mecânico.

Caixa Postal: 6051-13083-970, Telefone: (021)-(055)-(19)-37883178, Fax: (021)-(055)-(19)-32893722.

abdon@fem.unicamp.br.

**Katia Lucchesi Cavalca.**

UNICAMP - Universidade Estadual de Campinas, Departamento de Projeto Mecânico.

Caixa Postal: 6051-13083-970, Telefone: (021)-(055)-(19)-37883183, Fax: (021)-(055)-(19)-32893722.

katia@fem.unicamp.br.

**Abstract.** *Frequently, when a mechanical system is projected, it is necessary to have a representative mathematical model of the system, for the purposes of prediction of the dynamic behavior of the system, so much under different operation conditions, as under different geometric conditions and different physical properties for each one of the components of the system. In this work, the sensitivity analysis is carried out to the selection of the best mathematical model to represent the mechanical couplings. Soon afterwards, this model is validated, through adjustment of the experimental data, obtained for flexible couplings of metallic disk type, with different dimensions and physical properties. The mathematical model is implemented using the method of finite elements to represent each one of the components of the system, and the models of the couplings are simplified in agreement with the related literature. Only the vibrations in the transversal plane are considered.*

**Keywords:** *flexible coupling, frequency response function, sensitivity analysis.*

### 1. Introduction.

The application of flexible couplings in mechanical rotating systems is currently very large, due to the considerably variety of types to these components, which tends to increase as well as the technological development rises. The main factors to cause technological development are design proposals involving new materials and possibilities of obtaining several solutions for geometric configurations of these components, as well as different possibilities of assembling.

Therefore, the implementation of mathematical models that represent the mechanical couplings and their validation is not so usual. Among the first proposals of modeling there are the works developed by Nelson and Crandall (1992), Kramer (1993), which presented equivalent models based in stiffness and damping coefficients. Some studies for implementation and validation of these models can be found in Tapia (2003), Tapia e Cavalca (2003, 2004).

In this way, the main contribution of the present work is the technical information added to the previous publications, as the sensitivity analysis of the finite elements model to the rotor-coupling system related to the mathematical coupling models proposed to represent the flexible couplings. A quite simple experimental test condition is considered with the purpose of getting a system where the unique parameters to be evaluated are those corresponding to the couplings. This procedure enables the analysis to avoid considerably influence of other components in the fitting process. Three different types of flexible couplings are described in the experimental tests. The couplings are manufactured by Vulkan of Brazil as metallic flexible disks couplings.

### 2. The Mechanical System.

Figure 1 shows the inertial and auxiliary reference systems to the rotor-haft system. In this work, only the bending vibrations of the system are considered. An inertial reference system  $XYZ$  and an auxiliary reference system  $xyz$ , fixed in the shaft, describe the equations of motion of the system. A generic cross section of the bending rotor is defined regarding the system  $XYZ$  through the generalized coordinates  $(u, v, \alpha, \beta)$ .  $u(Y, t)$ ,  $v(Y, t)$  are the translations in  $X$  and  $Z$  directions, which supply the cross section centre position at the instant  $t$ .  $\alpha(Y, t)$  and  $\beta(Y, t)$  supply the orientation of the cross section around  $X$  and  $Z$  axes respectively.

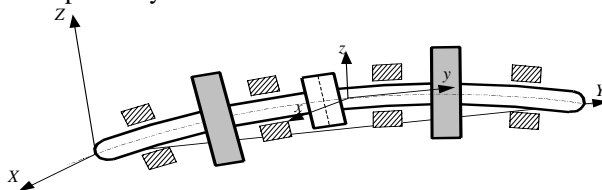


Figure 1. Mechanical Systems.

### 3. Mechanical Couplings.

According to Tapia (2003), there are few simplified models to represent mechanical couplings in Rotor-Coupling-Bearing Systems. Therefore, there is less discussion about what simplified model can be the best representation for the physical problem involving the mechanical axial coupling (rigid or flexible).

#### 3.1. Second Model of Kramer

The second model implemented, according to Kramer (1993), takes into account the stiffness  $k_R$  and the damping  $c_R$  of the coupling. In this case, the coupling effect consists in constraining the translation degrees of freedom before node  $i$  and after node  $j$  of the coupling ( $u_i=u_j$  and  $v_i=v_j$ ), according to Fig. 2.

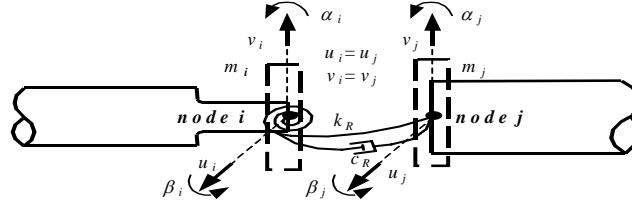


Figure 2. The 2<sup>nd</sup> model implemented for the flexible coupling.

#### 3.2. Nelson and Crandall Models

The first model implemented takes into account the considerations stated by Nelson and Crandall (1992). This model represents the coupling as an elastic component with isotropic translational stiffness  $k_T$  and rotational stiffness  $k_R$ , between the stations  $i$  and  $j$ , corresponding to the connecting points of the shafts, as shown in Fig. 3a. The second model is also according to the considerations stated by Nelson and Crandall (1992). This model considers stiffness and damping of the coupling, through both translational and rotational equivalent stiffness and damping coefficients ( $k_T$ ,  $k_R$ ,  $c_T$ ,  $c_R$ ) according to Fig. 3b.

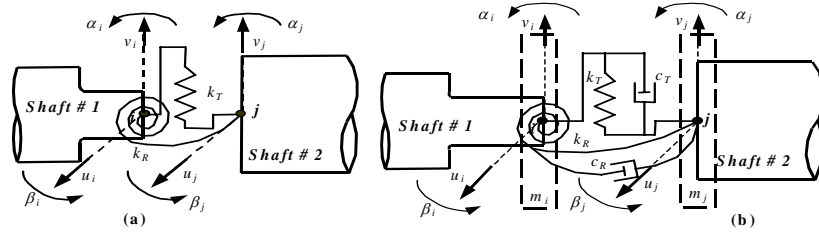


Figure 3. Nelson and Crandall Models: (a) 1<sup>st</sup> Model; (b) 2<sup>nd</sup> Model.

In the models presented, the inertia effects are included considering two rigid disks located in both stations of the shafts connection. The equation of motion of the coupling, for each model previously described is written in the following form:

$$[M_a] \begin{Bmatrix} \ddot{q}_i \\ \ddot{q}_j \end{Bmatrix} + [\mathcal{Q}[G_a] + [C_a]] \begin{Bmatrix} \dot{q}_i \\ \dot{q}_j \end{Bmatrix} + [K_a] \begin{Bmatrix} q_i \\ q_j \end{Bmatrix} = \{F_{ex}\} + \{F_{con}\}. \quad (1)$$

Where:

- $\{F_{con}\}, \{F_{ex}\}$  are the connecting forces and external forces vectors, acting on the coupling;
- $[M_a], [G_a]$  are the mass and gyroscopic matrices due to the coupling, similar to those for the rigid disks (rotors);
- $[C_a], [K_a]$  are the damping and stiffness matrices due to the coupling. The damping matrix can be null depending on the model considered (Tapia, 2003).

These physical coupling models are isotropic models of mass-spring-damper systems, in which low values of translational and/or rotational stiffness coefficients approach the dynamical behavior of flexible couplings, as well high values of the same parameters simulate approximately rigid coupling.

#### 4. Sensitivity Matrix of the Frequency Response Functions

Duarte M.A.V. (1994) defined sensitivity of frequency response functions by using the first order finite differences, applying the partial derivatives of the *FRFs* related to the structural parameters of the rotor. Tapia (2003) gives the FRF matrix for a rotating system, using the mechanical impedance matrix:

$$[H(\omega)] = [-\omega^2 [M_g] + i\omega [\mathcal{Q}[G_g] + [C_g] + [CV_g]] + [K_g]]^{-1} \quad (2)$$

Where:  $\omega$  is the frequency of the excitation force;  $[M_g]$ ,  $[C_g]$ ,  $[K_g]$ ,  $[G_g]$  are the global matrices of mass, damping, stiffness, and gyroscopic matrix of the system;  $[CV_g]$  is the proportional viscous damping matrix of the system.

The sensitivity of any *FRF* related to a parameter  $p_k$ , using the derivative property of the inverse matrix, is defined by:

$$\frac{\partial[H(\omega)]}{\partial p_k} = -[[IM]^{-1}] \frac{\partial[IM]}{\partial p_k} [IM]^{-1}, \text{ with: } [IM(\omega)] = -\omega^2 [M_g] + i\omega [\mathcal{Q}[G_g] + [C_g] + [CV_g]] + [K_g] \quad (3)$$

$$\text{Where: } \frac{\partial[IM(\omega)]}{\partial p_k} = -\omega^2 \frac{\partial[M_g]}{\partial p_k} + i\omega \left[ \mathcal{Q} \frac{\partial[G_g]}{\partial p_k} + \frac{\partial[C_g]}{\partial p_k} + \frac{\partial[CV_g]}{\partial p_k} \right] + \frac{\partial[K_g]}{\partial p_k}.$$

For a FRF  $H_{ij}(\omega)$ , an element of the sensitivity matrix  $[S]_{pt \times np}$  is defined by:

$$S_{lk} = \frac{\partial H_{ij}(\omega_l)}{\partial p_k}; \text{ with: } l = 1, \dots, pt; k = 1, \dots, np \text{ (} pt : \text{number of points of FRF; } np : \text{number of parameters)} \quad (4)$$

The derivatives presented in Eq. (3) can be obtained analytical or numerically, which means a certain difficulty level, depending on modeled complexity. Therefore, the sensitivity matrix is defined by finite differences, applying the Brown and Dennis rules (Duarte M. 1981), as follow:

$$S_{lk}(\omega_l) = \frac{H_{ij}(\omega_l)|_{p_k + \Delta p_k} - H_{ij}(\omega_l)|_{p_k}}{\Delta p_k}; \Delta p_k = \begin{cases} 10^{-9} & \text{if } |p_k| < 10^{-6} \\ 10^{-3}|p_k| & \text{if } |p_k| \geq 10^{-6} \end{cases} \text{ with: } l = 1, \dots, npt; k = 1, \dots, np \quad (5)$$

The sensitivity coefficient can be normalized with respect to the parameter value and to the transfer function value, as follow:

$$NS_{lk} = \frac{p_k}{H_{ij}(\omega_l)} \frac{\partial H_{ij}(\omega_l)}{\partial p_k}, \text{ where: } NS \text{ normalized coefficient.} \quad (6)$$

#### 5. The Experimental System.

The system showed in Fig. 4 represents the rotor-coupling model used to apply the process of sensitivity analysis of the coupling model in the mechanical system. The system is composed by two shafts and one coupling between them.

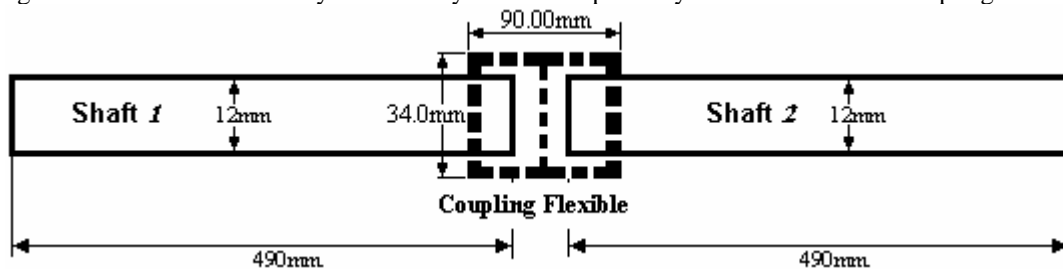


Figure 4. Rotor-Coupling Experimental System.

Tab. 1, Tab. 2 and Tab.3 show the dynamic and physical characteristics of shaft and disk couplings that were used in the mechanical system, for each experimental testing. These parameters were estimated through adjust process for each shaft, using modal analysis under free-free condition. However, these values are the mean of the evaluated values. The values of three couplings used were giving for Vulkan of Brazil factory and the others were calculated to consider the effect of inertia of the flexible coupling.

Table 1. Properties of the shafts.

Shafts	Density	Young Modulus	Poisson coefficient	Shear factor	Viscous damping factors:
	7759.255kg/m <sup>3</sup>	2.000*10 <sup>11</sup> N/m <sup>2</sup>	0.3	0.9	$q_{zk}=609.009*10^{-9}$ , $q_{zm}=529.571^{-3}$

Table 2. Technical characteristic and data of coupling Vulkan Tormin L-3R.


	Technical data	Assumed Values
	Moment of Torsion = 40.0Nm. Max rotation = 13900.0rpm. Mass = 0.961kg. Inertia moment = $0.044^{-2} \cdot 10 \text{kgm}^2$ . Cub material = Nodular iron. Disk material = Steel (1.0mm).	Equivalent density = $78.078 \cdot 10^{-7} \text{kg/mm}^3$ . Equivalent thickness = 31.5mm. Inner radius = 6.0mm. Outer radius = 34.5mm.

Table 3. Technical characteristic and data of coupling Vulkan Tormin L-1R.



	Technical data	Assumed Values
	Moment of Torsion = 4.0Nm. Max rotation = 13900.0rpm. Mass = 0.112kg. Cub material = Aluminum. Disk material = Steel (0.5mm).	Equivalent density = $298.080 \cdot 10^{-8} \text{kg/mm}^3$ . Equivalent thickness = 29.5mm. Inner radius = 6.0mm. Outer radius = 22.0mm.

Table 4. Technical characteristic and data of coupling Vulkan Tormin L-1NZ.

	Technical data	Assumed Values
	Moment of Torsion = 4.0Nm. Max rotation = 2000.0rpm. Mass = 0.129kg. Cub material = Aluminum. Disk material = Steel (0.5mm).	Equivalent density = $244.840 \cdot 10^{-8} \text{kg/mm}^3$ . Equivalent thickness = 37.5mm. Inner radius = 6.0mm. Outer radius = 22.0mm.

### 5.1. Finite Element Model for experimental assembly

Figure 5 illustrates the experimental assembly of the rotor-coupling system to the acquisition of the FRFs of the system. Otherwise, the three finite element models for the couplings are showed. In the scheme, point  $F$  represents the driving point (application of the external excitation force) and  $R_i$  represent the acquisition points where the FRFs were measured.

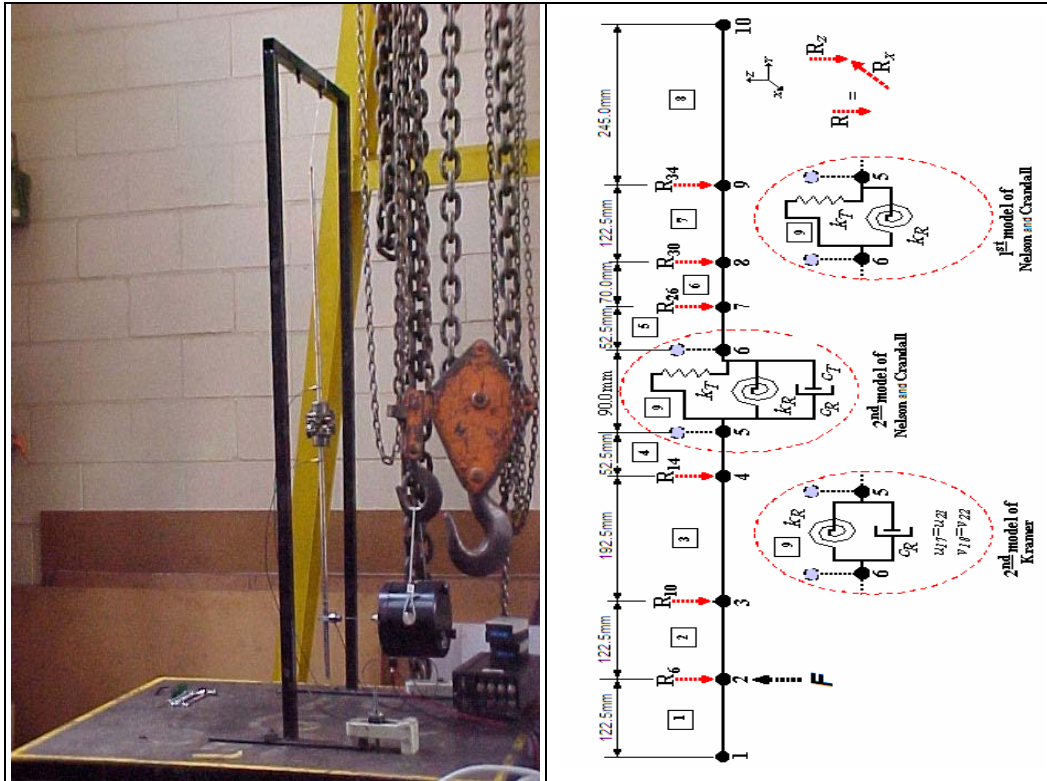


Figure 5. Set-up experimental and finite element model of the system.

## 5.2. The Analysis Process.

The analysis process used on this work, after obtain the experimental frequencies response functions, for each one of the couplings (Tormin L3R, Tormin L1R, Tormin L1NZ) is described as follow:

- On a first stage, a very simplified adjust has been made, using the model with more parameters (2<sup>nd</sup> Nelson Crandall 1993), on the purpose to estimate values of stiffness and damping parameters.
- As results of this process, it is obtained a range of values for each one of the parameters, the same ones presented on Tab. 5.

Table 5. Value range of couplings stiffness and damping parameters.

$\omega$ : Hz	$K_T$ : N/m		$K_R$ : Nmm/rad		$C_T$ : Ns/m		$C_R$ : Nms/rad	
400.00	Minimum	Maximum	Minimum	Maximum	Minimum	Maximum	Minimum	Maximum
1000.00	100.00	$160.00 \cdot 10^5$	0.100	$148.00 \cdot 10^2$	0.95	12.70	$0.95 \cdot 10^{-7}$	0.73

- On a next stage, once determined the range of values for each one of the parameters which represent the coupling, it was followed the sensitivity analysis of the frequencies response functions on the degrees of freedom on the finite element model, which the experimental frequencies response functions were obtained, selecting a range of exciting frequencies.

Figure 6 shows the behavior of the normalized sensitivity of FRF (frequency response function) on a degree of freedom, related to the parameters of stiffness  $K_T$  e  $K_R$  considering the 2<sup>nd</sup> model.

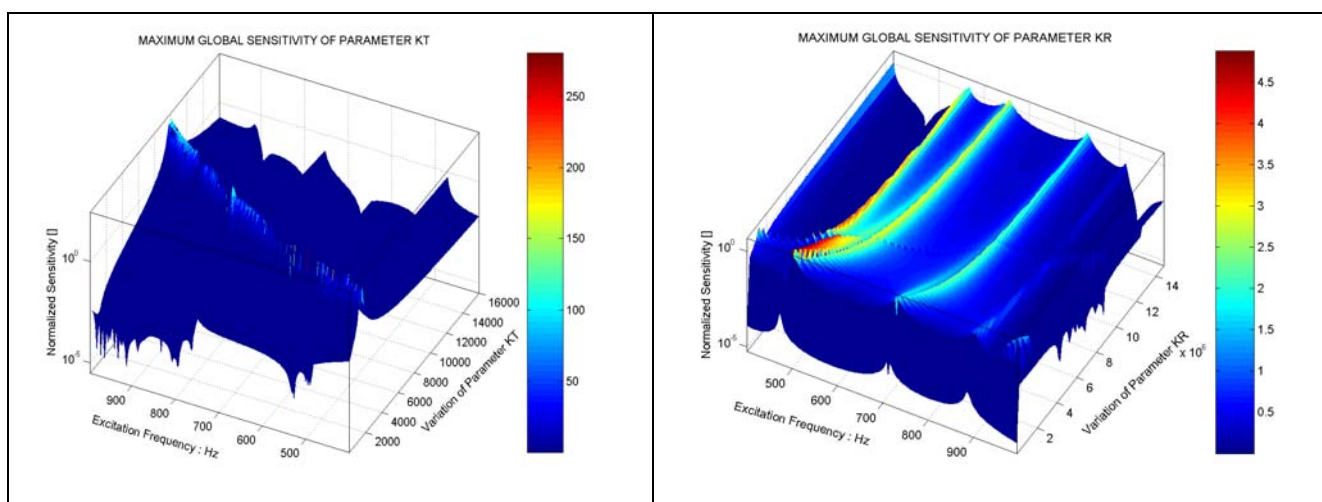


Figure 6. Normalized sensitivity of FRF to the parameter  $K_T$  and  $K_R$  for to 2nd model (Nelson and Crandall).

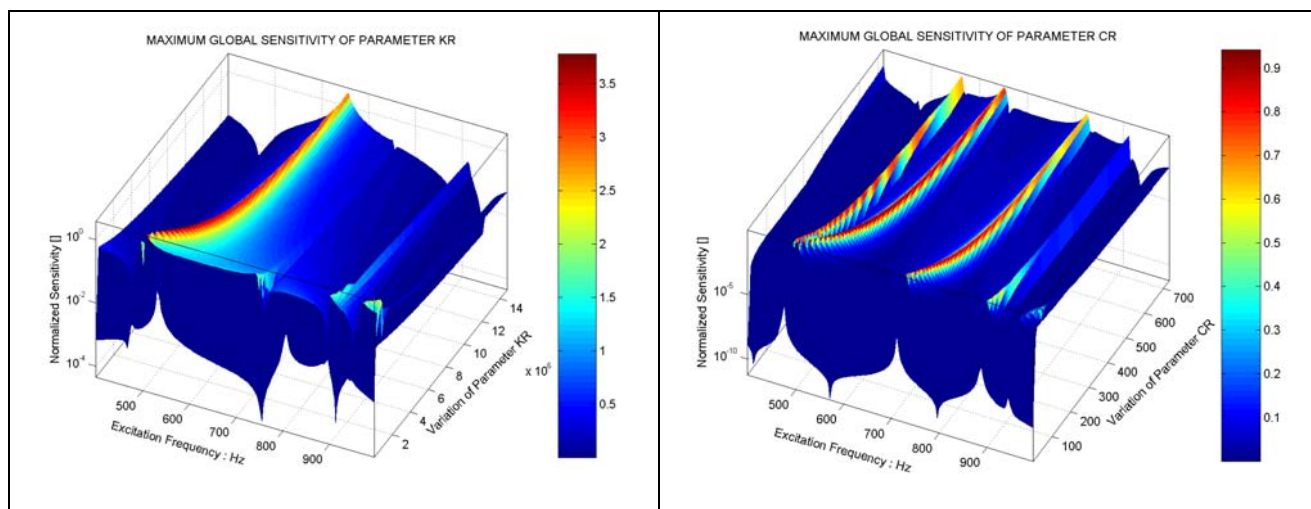


Figure 7. Normalized sensitivity of FRF to the parameter  $K_R$  and  $C_R$  for to 2nd model (Kramer).

Figure 7 shows the behavior of the normalized sensitivity of FRF (frequency response function) on a degree of freedom, related to the parameters of stiffness and damping  $K_R$  e  $C_R$  considering the 2<sup>nd</sup> model (Kramer).

The normalized sensitivity of the FRF was calculated using the Eq. (6), for each one of the degrees of freedom considered and for each one of the three implemented coupling models. The Tab. 5, shows the percent values of obtained sensitivity. These values were estimated using the Eq. (7).

$$\left( \sum NS_{ik} / NS_{\max} \right) * 100\%, \text{ where : } NS_{\max} \text{ normalized coefficient maximum} \quad (7)$$

Table 5. Normalized Sensitivity of each degree of freedom (d.o.f)

Degree of freedom	2nd. Nelson Crandall				1st. Nelson Crandall		2nd. Kramer	
	$\partial H / \partial K_T$	$\partial H / \partial K_R$	$\partial H / \partial C_T$	$\partial H / \partial C_R$	$\partial H / \partial K_T$	$\partial H / \partial K_R$	$\partial H / \partial K_R$	$\partial H / \partial C_R$
6	59.99%	100.00%	61.57%	100.00%	88.72%	100.00%	100.00%	100.00%
10	61.37%	39.28%	60.71%	43.28%	64.13%	65.17%	39.32%	43.79%
14	79.84%	68.41%	78.20%	74.61%	86.64%	84.26%	68.04%	73.90%
26	100.00%	70.95%	100.00%	61.11%	100.00%	65.69%	68.64%	60.23%
30	58.32%	71.06%	56.23%	59.40%	62.86%	64.57%	68.06%	58.62%
34	78.27%	71.45%	71.22%	59.78%	79.81%	65.03%	68.10%	58.56%

Observing the values on Tab. 5, the FRFs determined on each 26 and 6 degrees of freedom are the most sensitive to the variation of coupling's parameters of stiffness and damping to the different considering models.

After established the most sensitive degrees of freedom, the follow step was to adjust the experimental FRFs determined for each one of the three flexible disk couplings, considering those degrees of freedom.

Figure 8 shows the result of the adjust process for the experimental FRFs obtained for Tormin L3R, Tormin L1R and Tormin L1NZ couplings, on the 6 and 26 degrees of freedom in this system, considering for each coupling the 2<sup>o</sup> model of Nelson and Crandall. The FRF considered is the inertance on an exciting frequency range of 450.0Hz to 700.0Hz.

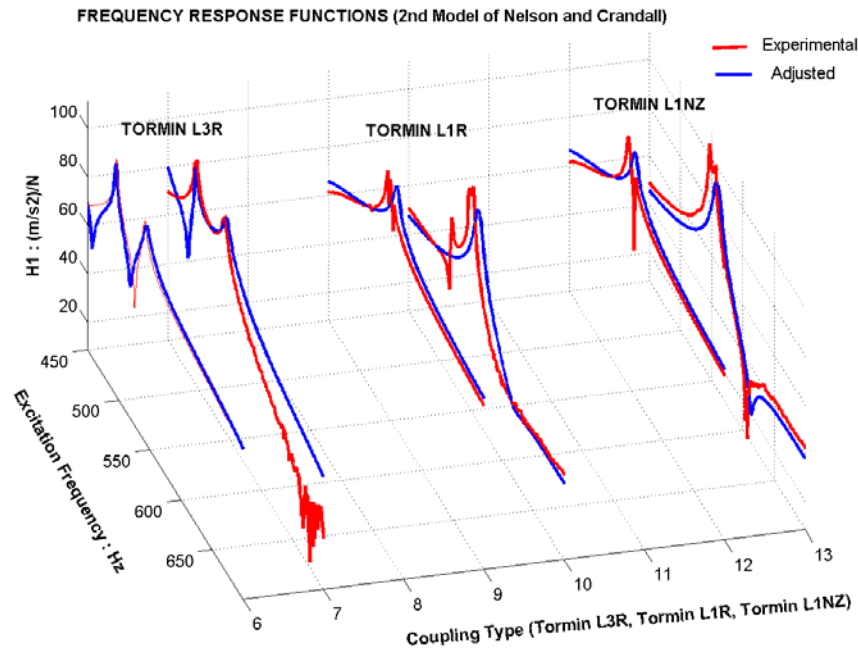


Figure 8. Results of adjusted process to 2nd Model of Nelson Crandall.

Figure 9 shows the adjust process results for the experimental FRFs obtained for the same three tested couplings experimentally, also on the 6 and 26 degrees of freedom in the system and on the same exciting frequency range of 450.0Hz a 700.0Hz. Although, on this case, it was considered the 1<sup>o</sup> Model of Nelson and Crandall to represent the coupling in all the analysis performed.

Finally, Figure 10 shows the adjust process results, for the experimental FRFs obtained for the same three tested couplings experimentally, also on the 6 and 26 degrees of freedom in the system and on the same exciting frequency



range of 450.0Hz to 700.0Hz. This time, it was considered the 2<sup>o</sup> Model of Kramer to represent the coupling in all the analyzed cases.

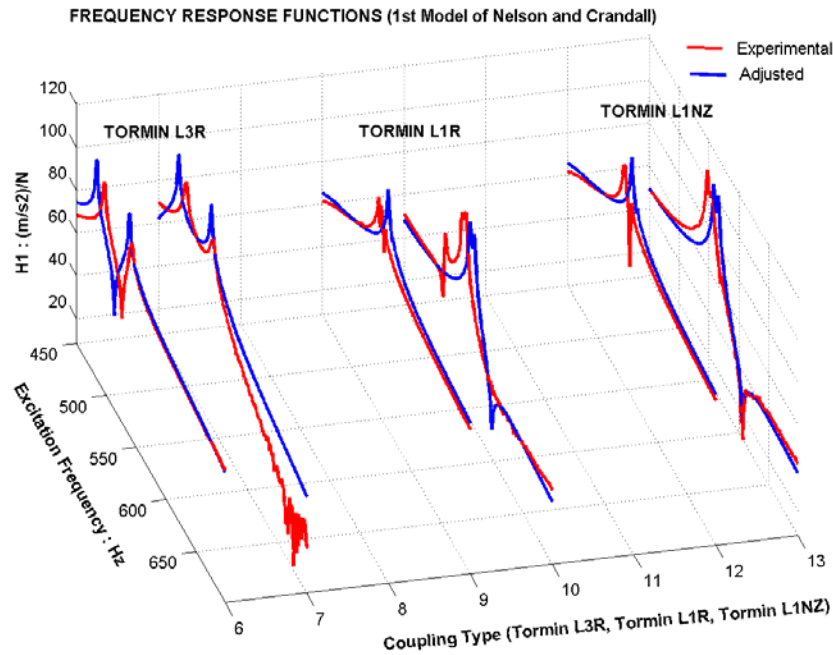


Figure 9. Results of adjusted process to 1st Nelson Crandall.

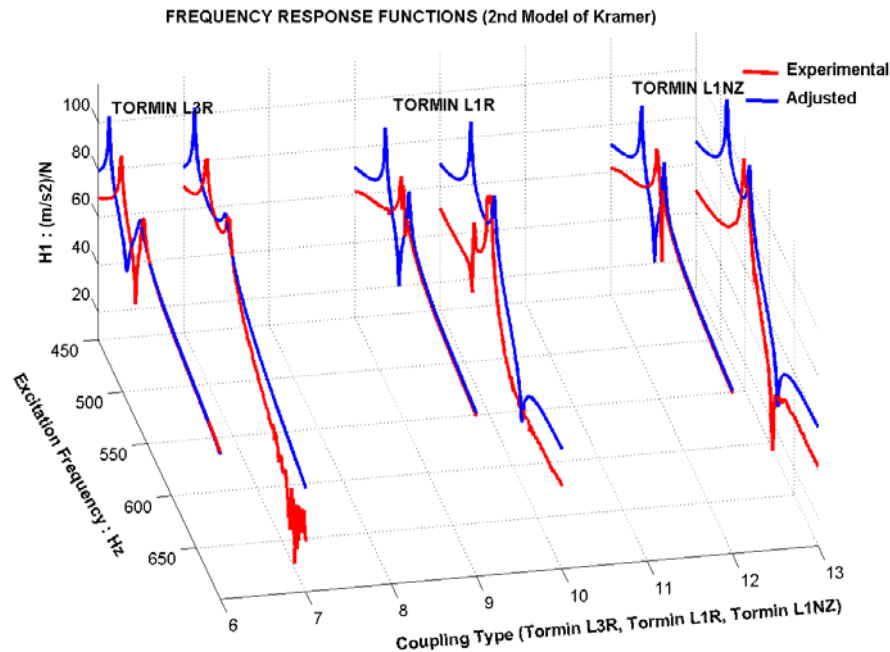


Figure 10. Results of adjusted process to 2nd Model of Kramer.

The results obtained on the different adjust process accomplished on this present work are presented on Tab. 6. It is indicated the convergence of the values for each one of the parameters of stiffness and damping which represent mathematically the coupling for each one of the experimented models. Even though, it was presented the percent average errors in each case. The average error for each adjust process was calculated according to Eq. (8).

$$erro\ medio = \left( \sum_{i=1}^n \frac{|H_{exp} - H_{adj}|}{H_{exp}} * 100\% \right) / n. \quad (8)$$

Where:  $H_{exp}$  is the experimental FRF;  $H_{adj}$  is the FRF obtained with the finite element model of the system after the adjustment and  $n$  is the number of points on each FRF considered on the process.

Table 6. Results of the adjust process to each three coupling model.

Type of Coupling	2nd. Nelson Crandall				1st. Nelson Crandall		2nd. Kramer	
	$K_T$ :N/m	$K_R$ :Nm/rad	$C_T$ :Ns/m	$C_R$ :Nms/rad	$K_T$ :N/m	$K_R$ :Nm/rad	$K_R$ :Nm/rad	$C_R$ :Nms/rad
Tormin L3R	$202.044 \cdot 10^4$	$121.182 \cdot 10^1$	4.650	0.020	$155.851 \cdot 10^4$	$106.073 \cdot 10^3$	$100.182 \cdot 10^1$	0.025
Tormin L1R	$256.908 \cdot 10^2$	17.903	59.182	0.024	$595.053 \cdot 10^2$	28.370	$0.001 \cdot 10^{-2}$	0.002
Tormin L1NZ	$275.978 \cdot 10^1$	1.078	15.500	0.001	$627.250 \cdot 10^2$	15.486	$0.004 \cdot 10^{-9}$	0.001
	Mean Error %				Mean Error %		Mean Error %	
	d.o.f: 6		d.o.f: 26		d.o.f: 6	d.o.f: 26	d.o.f: 6	d.o.f: 26
Tormin L3R	4.46%		30.23%		6.26%	27.93%	7.42%	27.64%
Tormin L1R	4.71%		10.72%		5.11%	10.60%	8.18%	39.37%
Tormin L1NZ	4.59%		13.89%		5.04%	9.23%	8.06%	41.52%

## 6. Conclusions.

Nelson and Crandall's second model had the best performance on the adjustment process for the experimental data obtained with the three flexible disk couplings, confirming what was observed on the graphics of sensitivity presented. The first model of Nelson and Crandall does not present the same representative degree that the second model for all cases, what can be confirmed for the average error values on different adjustment process shown on Tab. 6. Kramer's second model had a low performance on the adjustment process for all cases, which is visualized on diagrams of sensitivity, as on the average errors presented on Tab. 6. Although, this fact could be justified in function of the analyzed range, which could be more sensitive to translational parameters of stiffness and damping than to rotational parameters of stiffness and damping. According to Figs. 8, 9 and 10, the models L1R and L1NZ present some discrepancies in the FRFs fitting. Such difference maybe can be explained by the highest damping effect in these couplings due to their greatest flexibility characteristic. Anyway, this fact must be more investigated in future research. Finally, it can be concluded that all the three experimented coupling could be better represented for models which consider parameters of stiffness and damping, both in translational and rotational directions.

## 7. Acknowledgements.

The authors thank CNPq, FAPESP, CAPES, VULKAN do Brasil and UNICAMP for supporting this work.

## 8. References.

- Kramer, E., 1993, "Dynamics of Rotors and Foundations", New York, Springer-Verlag. pp. 381.
- Nelson, H. D., Crandall, S. H., 1992, "Analytic Prediction of Rotordynamic Response". In: EHRICH, F. F., Handbook of Rotordynamics. United States of America, McGraw-Hill, Inc., Cap.2, pp. 2.1-2.84.
- Arruda, J. R. F., 1987, "Rotor finite element model adjusting". In: Proceedings of the 9<sup>th</sup> Brazilian Congress of Mechanical Engineering, Florianópolis, SC, pp.741-744.
- Arruda, J. R. F., 1989, "Rotor model adjusting by unbalance response curve-fitting". In: Proceedings of the 7<sup>th</sup> International Modal Analysis Conference, v.1, Society for Experimental Mechanics, pp.479-484.
- Duarte, M. V., 1994, "Ajuste de modelos dinâmicos de estruturas com não linearidades concentradas". Campinas: Faculdade de Engenharia Mecânica, Universidade Estadual de Campinas, 190p., Tese (Doutorado).
- Tapia, A. T., 2003, "Modelagem dos Acoplamentos Mecânicos nos Sistemas Horizontais Rotor-Acoplamento-Mancal". Campinas: Faculdade de Engenharia Mecânica, Universidade Estadual de Campinas, 250p. Tese (Doutorado).
- Tapia, A. T.; Cavalca, K. L., 2003, "Ajuste de Parâmetros dos Modelos de Acoplamentos Flexíveis nos Sistemas Rotor-Acoplamento-Mancal Usando as Funções de Resposta em Frequência": XVII Congresso Brasileiro de Engenharia Mecânica (COBEM2003), São Paulo-Brasil, Novembro de 2003.
- Tapia, A. T.; Cavalca, K. L., 2004, "Evaluation of Rigid and flexible Coupling Models in na Experimental Rotor-Coupling-Bearing system Using Frequency response Functions". VIII International Conference on Vibration in Rotating Machinery (I Mech E 2004), Swansea Inglaterra, Setembro de 2004.

## 9. Responsibility notice

The authors are the only responsible for the printed material included in this paper.